PHYSICAL REVIEW D **85,** 075008 (2012)

Two-Higgs-doublet model and double-lepton polarization asymmetries in $B \to K_0^*(1430)\ell^+\ell^-$ decay

F. Falahati[1,*] and R. Khosravi[2,†]

[1]*Physics Department, Shiraz University, Shiraz 71454, Iran*
[2]*Department of Physics, Isfahan University of Technology, Isfahan 84156-83111, Iran*

(Received 11 October 2011; published 6 April 2012)

In this paper, the dependency of P_{ij}'s on the dilepton invariant mass, q^2, and the model III two-Higgs-doublets model (2HDM) parameters for $B \to K_0^*(1430)\ell^+\ell^-$ decay were investigated, and the results were compared to those of the standard model (SM) and Appelquist, Cheng and Dobrescu model. Also, for this decay, the effects of model III 2HDM parameters on the averages of double-lepton polarization asymmetries, $\langle P_{ij}\rangle$'s, were studied, and by taking into account the corresponding theoretical and experimental errors in the SM, the results of the SM and 2HDM were compared to each other. In addition, by comparing the averages of double-lepton polarization asymmetries in 2HDM to those of SM4 and obtaining the required number of events for detecting each asymmetry at the LHC or the Super Large Hadron Collider, we present a comprehensive discussion regarding the lepton polarizations of $B \to K_0^*\ell^+\ell^-$ decay. We discovered that the study of the double-lepton polarization asymmetries and the corresponding averages in the $B \to K_0^*(1430)\ell^+\ell^-$ decay can provide good signals for probing new physics beyond the SM in the future B-physics experiments.

DOI: 10.1103/PhysRevD.85.075008 PACS numbers: 12.60.−i, 13.30.−a, 14.20.Mr

I. INTRODUCTION

The decays induced by lepton-flavor violating transitions or caused by flavor-changing neutral current (FCNC) transitions provide an excellent testing ground for the standard model (SM). These decays which are suppressed in the SM at tree level arise at loop level and are very sensitive to the gauge structure of the SM. Moreover, these decays are also quite sensitive to the existence of new physics beyond the SM, since either loop processes with new particles [1–7] or allowed new diagrams at tree level [8–10] can give considerable contribution to rare decays. Among these, the rare B-meson decays, which take place via the FCNC, including $b \to s(d)$ transition, play a distinctive role in both experimental measurements and theoretical studies for the precision test of the SM and for searching new physics beyond the SM.

Although most experiments are in agreement with the SM predictions, it is widely believed that the SM cannot be the final theory of particle physics and merely could be an effective theory at the electroweak scale, in particular, because the Higgs sector of the SM is not well-understood yet, and the cause of neutrino oscillations, matter-antimatter asymmetry, and the nature of dark matter are not explicitly explained in the SM. As a result, for understanding these phenomena, new physics beyond the SM should be included. Some possible extensions of the SM are the little Higgs model [11,12], extra dimensions [13,14], and multi-Higgs models like the minimal supersymmetric standard model [15], which are extensively explored by many reseachers. One of the most popular extensions of the SM is two-Higgs-doublets model (2HDM) in which two complex Higgs doublets are considered, contrary to the SM which contains only one. In general, in 2HDM, the FCNCs that happen at tree level are eliminated by imposing an *ad hoc* discrete symmetry [16]. One possible approach to keeping neutral flavor conservation at tree level is to couple all fermions to only one of the aforementioned Higgs doublets (model I). Another possibility is the coupling of the up-type quarks to the first Higgs doublet and down-type quarks to the second Higgs doublet (model II). Model II is more popular because its Higgs sector coincides with the ones in the supersymmetric model. The physical content of the Higgs sector, which is model independent, includes five physical Higgs fields: neutral scalars H^0, h^0; neutral pseudoscalar A^0; and charged Higgs bosons $H^\pm$. The interaction vertex of fermions with Higgs fields depend on $\tan\beta = \upsilon_2/\upsilon_1$, where υ_1 and υ_2 are the vacuum expectation values of the two Higgs doublets. The constraints on the charged Higgs boson mass and $\tan\beta$ are usually obtained by using experimental results for the branching ratio of $b \to s\gamma$ and $B \to D\tau\bar{\nu}_\tau$ decays as well as $B - \bar{B}$ and $K - \bar{K}$ mixing in the literature[17]. Without considering discrete symmetry, a more general form of 2HDM, namely, model III has been obtained, which allows for the presence of FCNC at tree level. Consistent with the low energy constraints, the FCNCs involving the first two generations are highly suppressed, and those involving the third generation are not as severely suppressed as the first two generations. Also, in such a model, there exists rich induced CP-violating sources from a single CP phase of vacuum that is absent in the SM, model I, and model II.

*falahati@shirazu.ac.ir
†khosravi.reza@gmail.com

 © 2012 American Physical Society

One efficient way for discovering new physics is the measurement of lepton polarization in the semileptonic decays of B which has been widely discussed in the literature [1–7,18–20]. Based on this, the aim of the present work is to derive quantitative predictions for the double-lepton polarization asymmetries in the exclusive $B \to K_0^*(1430)\ell^+\ell^-$ decay, in the context of the general two-Higgs-doublet model with spontaneous CP violation (model III). We also suppose that all tree level FCNC couplings are negligible. The constraints on the phase angle θ in the product $\lambda_{tt}\lambda_{bb}$ of Higgs-fermion coupling and the magnitudes of λ_{tt} and λ_{bb} come from the experimental results of the electric dipole moments of electron and neutron, $B^0 - \bar{B}^0$ mixing, ρ_0, R_b, $\Gamma(b \to s\gamma)$, and $\Gamma(b \to c\tau\bar{\nu}_\tau)$ [21–24]. It is also worth noting that the effects of two other new physics models beyond the SM, SM4 [6] and Appelquist, Cheng and Dobrescu model (ACDM) [25], have recently been investigated on the same asymmetries of $B \to K_0^*(1430)\ell^+\ell^-$ decay, which have been discussed in this work; we have also compared the results of this paper to the results of Refs. [6,25].

This paper is organized as follows. In Sec. II, we first present the expressions for the matrix elements of B to a scalar meson, here $B \to K_0^*(1430)\ell^+\ell^-$, in SM and 2HDM. Then, the general expressions for the double-lepton polarization asymmetries have been extracted out. The sensitivity of these polarizations and the corresponding averages to the model III 2HDM parameters have been numerically analyzed in Sec. III. In the final section, a summery of concluding remarks is presented.

II. THE MATRIX ELEMENT AND DOUBLE-LEPTON POLARIZATIONS OF $B \to K_0^*\ell^+\ell^-$ IN SM AND 2HDM

The QCD-corrected effective Hamiltonian for the decay $B \to K_0^*\ell^+\ell^-$, which is described by the $b \to s\ell^+\ell^-$ transition at quark level in the general 2HDM, can be written as [26]

$$\mathcal{H}_{\text{eff}} = -\frac{4G_F}{\sqrt{2}} V_{tb}V_{ts}^*\Big\{\sum_{i=1}^{10} C_i(\mu)O_i(\mu) + \sum_{i=1}^{10} C_{Q_i}(\mu)Q_i(\mu)\Big\}, \tag{1}$$

where the first set of operators in the curly brackets is related to the effective Hamiltonian in the SM, and the corresponding Wilson coefficients are modified by considering the contributions of charged Higgs diagrams. The explicit forms of these operators and the corresponding Wilson coefficients C_i can be found in Ref. [27]. The second set of operators in the brackets, whose explicit forms are presented in Ref. [26], originate from the neutral Higgs bosons exchange diagrams. The corresponding Wilson coefficients at scale $\mu \simeq m_W$ are

$$C_{Q_1}(m_W) = \frac{m_b m_\ell}{m_{h^0}^2}\frac{1}{|\lambda_{tt}|^2}\frac{1}{\sin^2\theta_W}\frac{x}{4}\{(\sin^2\alpha + h\cos^2\alpha)f_1(x,y) + \Big[\frac{m_{h^0}^2}{m_W^2} + (\sin^2\alpha + h\cos^2\alpha)(1-z)\Big]f_2(x,y) + \frac{\sin^2 2\alpha}{2m_{H^\pm}^2}\Big[m_{h^0}^2 - \frac{(m_{h^0}^2 + m_{H^0}^2)^2}{2m_{H^0}^2}\Big]f_3(y)\Big\}, \tag{2}$$

$$C_{Q_2}(m_W) = -\frac{m_b m_\ell}{m_{A^0}^2}\frac{1}{|\lambda_{tt}|^2}\Big\{f_1(x,y) + \Big[1 + \frac{m_{H^\pm}^2 - m_{A^0}^2}{m_W^2}\Big]f_2(x,y)\Big\}, \tag{3}$$

$$C_{Q_3}(m_W) = \frac{m_b e^2}{m_\ell g^2}[C_{Q_1}(m_W) + C_{Q_2}(m_W)], \tag{4}$$

$$C_{Q_4}(m_W) = \frac{m_b e^2}{m_\ell g^2}[C_{Q_1}(m_W) - C_{Q_2}(m_W)], \tag{5}$$

$$C_{Q_i}(m_W) = 0 \qquad i = 5, \ldots, 10, \tag{6}$$

where

$$x = \frac{m_t^2}{m_W^2}, \qquad y = \frac{m_t^2}{m_{H^\pm}^2}, \qquad z = \frac{x}{y}, \qquad h = \frac{m_{h^0}^2}{m_{H^0}^2},$$

$$f_1(x,y) = \frac{x\ln x}{x-1} - \frac{y\ln y}{y-1},$$

$$f_2(x,y) = \frac{x\ln y}{(z-x)(x-1)} + \frac{\ln z}{(z-1)(x-1)},$$

$$f_3(y) = \frac{1 - y + y\ln y}{(y-1)^2}.$$

The QCD correction to the Wilson coefficients $C_i(m_W)$ and $C_{Q_i}(m_W)$ can be taken into account using the renormalization group equations. As it is discussed in Ref. [26], the operators O_9 and O_{10} do not mix with $Q_i (i = 1, \ldots, 10)$, so that the evolution of Wilson coefficients C_9 and C_{10} remain unchanged compared to their SM values.

In addition, the operators $O_i (i = 1, \ldots, 10)$ and $Q_i (i = 3, \ldots, 10)$ do not mix into Q_1 and Q_2, and also there is no mixing between Q_1 and Q_2. Therefore, the evolution of the coefficients C_{Q_1} and C_{Q_2} are performed by the anomalous dimensions of Q_1 and Q_2, respectively:

$$C_{Q_i}(m_b) = \eta^{-\gamma_Q/\beta_0} C_{Q_i}(m_W), \qquad i = 1, 2,$$

where $\gamma_Q = -4$ is the anomalous dimension of the operator $\bar{s}_L b_R$.

Now, using the aforementioned effective Hamiltonian, the one-loop matrix elements of $b \to s\ell^+\ell^-$ can be given in terms of the tree-level matrix elements of the effective operators as

$$\mathcal{M} = \langle s\ell^+\ell^-|\mathcal{H}_{\rm eff}|b\rangle$$
$$= -\frac{G_F\alpha}{2\sqrt{2}\pi}V_{tb}V_{ts}^*\{\tilde{C}_9^{\rm eff}\bar{s}\gamma_\mu(1-\gamma_5)b\bar{\ell}\gamma^\mu\ell + \tilde{C}_{10}\bar{s}\gamma_\mu(1-\gamma_5)b\bar{\ell}\gamma^\mu\gamma_5\ell - 2C_7^{\rm eff}\frac{m_b}{q^2}\bar{s}i\sigma_{\mu\nu}q^\nu(1+\gamma_5)b\bar{\ell}\gamma^\mu\ell$$
$$- 2C_7^{\rm eff}\frac{m_s}{q^2}\bar{s}i\sigma_{\mu\nu}q^\nu(1-\gamma_5)b\bar{\ell}\gamma^\mu\ell + C_{Q_1}\bar{s}(1+\gamma_5)b\bar{\ell}\ell + C_{Q_2}\bar{s}(1+\gamma_5)b\bar{\ell}\gamma_5\ell\}, \quad (7)$$

where q^2 is the invariant dileptonic mass, and the Wilson coefficients $C_7^{\rm eff}$, $\tilde{C}_9^{\rm eff}$, $\tilde{C}_{10}$, C_{Q_1}, and C_{Q_2} are calculated at the scale m_b. In order to obtain the effective coefficients $C_7^{\rm eff}$, $\tilde{C}_9^{\rm eff}$, and $\tilde{C}_{10}$ at the scale m_b, the values of coefficients C_7, $\tilde{C}_9$, and $\tilde{C}_{10}$ at the scale m_W are needed[1,26]. These coefficients, which are yielded from their SM values by adding the contributions due to the charged Higgs bosons exchange diagrams, are given by

$$C_7(m_W) = C_7^{\rm SM}(m_W) + |\lambda_{tt}|^2\left(\frac{y(7-5y-8y^2)}{72(y-1)^3} + \frac{y^2(3y-2)}{12(y-1)^4}\ln y\right) + \lambda_{tt}\lambda_{bb}\left(\frac{y(3-5y)}{12(y-1)^2} + \frac{y(3y-2)}{6(y-1)^3}\ln y\right), \quad (8)$$

$$\tilde{C}_9(m_W) = \tilde{C}_9^{\rm SM}(m_W) + |\lambda_{tt}|^2\left[\frac{1-4\sin^2\theta_W}{\sin^2\theta_W}\frac{xy}{8}\left(\frac{1}{y-1} - \frac{1}{(y-1)^2}\ln y\right) - y\left(\frac{47y^2-79y+38}{108(y-1)^3} - \frac{3y^3-6y^3+4}{18(y-1)^4}\ln y\right)\right], \quad (9)$$

$$\tilde{C}_{10}(m_W) = \tilde{C}_{10}^{\rm SM}(m_W) + |\lambda_{tt}|^2\frac{1}{\sin^2\theta_W}\frac{xy}{8}\left(-\frac{1}{y-1} + \frac{1}{(y-1)^2}\ln y\right). \quad (10)$$

It is observed from Eqs. (2), (3), and (8)–(10) that the SM results for the Wilson coefficients can be obtained from the corresponding coefficients in 2HDM by making the following replacements:

$$C_{Q_1} \to 0, \qquad C_{Q_2} \to 0, \qquad C_7^{\rm SM}(m_W) = C_7(y\to 0), \qquad \tilde{C}_9^{\rm SM}(m_W) = \tilde{C}_9(y\to 0), \qquad \tilde{C}_{10}^{\rm SM}(m_W) = \tilde{C}_{10}(y\to 0).$$

Note that the coefficient $\tilde{C}_9^{\rm eff}(\mu, q^2) \equiv \tilde{C}_9(\mu) + Y(\mu, q^2)$, where function Y contains the short-distance contributions from the one-loop matrix elements of the four quark operators, $Y_{\rm per}(q^2)$, as well as the long-distance effects associated with real $c\bar{c}$ in the intermediate states, $Y_{LD}(q^2)$. Therefore, $Y(q^2) = Y_{\rm per}(q^2) + Y_{LD}(q^2)$. The function $Y_{\rm per}(q^2)$ is given by

$$Y_{\rm per}(q^2) = g\left(\frac{m_c}{m_b}, s\right)(3C_1 + C_2 + 3C_3 + C_4 + 3C_5 + C_6) - \frac{1}{2}g(1,s)(4C_3 + 4C_4 + 3C_5 + C_6) - \frac{1}{2}g(0,s)(C_3 + 3C_4)$$
$$+ \frac{2}{9}(3C_3 + C_4 + 3C_5 + C_6), \quad (11)$$

where the explicit expressions for the g functions can be found in Ref. [28]. Y_{LD} is usually parameterized by using Breit-Wigner ansatz [29],

$$Y_{LD} = \frac{3\pi}{\alpha^2}C^{(0)}\sum_{V_i=\psi,\psi',\ldots}k_i\frac{\Gamma(V_i\to\ell^+\ell^-)m_{V_i}}{m_{V_i}^2 - q^2 - im_{V_i}\Gamma_{V_i}},$$

where α is the fine structure constant, and $C^{(0)} = (3C_1 + C_2 + 3C_3 + C_4 + 3C_5 + C_6)$. The phenomenological parameters k_i for the $B\to K^*(1430)\ell^+\ell^-$ decay can be fixed from $\mathcal{B}(B\to J/\psi K^*(1430)\to K^*(1430)\ell^+\ell^-) = \mathcal{B}(B\to J/\psi K^*(1430))\mathcal{B}(J/\psi\to\ell^+\ell^-)$. However, since the branching ratio of $B\to J/\psi K^*(1430)$ decay has not been measured yet, we assume that the values of k_i are in the order of 1. Therefore, we use $k_1 = 1$ and $k_2 = 1$ in the following numerical calculations.

From Eq. (7), it is obvious that, in order to calculate the decay width and other observables for the exclusive $B\to K_0^*(1430)\ell^+\ell^-$ channel, the matrix elements $\langle K_0^*(1430)|\bar{s}\gamma_\mu(1-\gamma_5)b|B\rangle$, $\langle K_0^*(1430)|\bar{s}i\sigma_{\mu\nu}\times q^\nu(1+\gamma_5)b|B\rangle$, and $\langle K_0^*(1430)|\bar{s}(1+\gamma_5)b|B\rangle$ have to be calculated. These matrix elements can be parametrized in terms of the form factors f^+, f^-, and f_T in the following way:

$$\langle K_0^*(1430)\mid\bar{s}\gamma_\mu(1-\gamma_5)b\mid B\rangle = -[f_+(q^2)(p_B + p_{K_0^*})_\mu + f_-(q^2)q_\mu], \quad (12)$$

$$\langle K_0^*(1430)\mid\bar{s}i\sigma_{\mu\nu}q^\nu(1\pm\gamma_5)b\mid B\rangle = \frac{\pm f_T(q^2)}{m_B + m_{K_0^*}}[(p_B + p_{K_0^*})_\mu q^2 - (m_B^2 - m_{K_0^*}^2)q_\mu], \quad (13)$$

where $q = p_B - p_{K_0^*}$ is the momentum transfer. To calculate the matrix element $\langle K_0^*(1430)|\bar{s}(1+\gamma_5)b|B\rangle$, we multiply both sides of Eq. (12) by q_μ and use the equation of motion. Finally, we get

$$\langle K_0^*(1430)\mid\bar{s}(1+\gamma_5)b\mid B\rangle = \frac{-f_0(q^2)}{m_b - m_s}, \quad (14)$$

where

$$f_0(q^2) = f_+(q^2)(m_B^2 - m_{K_0^*}^2) + q^2 f_-(q^2). \tag{15}$$

Using Eqs. (12)–(14), we obtain for the matrix element of the $B \to K_0^* \ell^+ \ell^-$ decay [30]

$$\begin{aligned}\mathcal{M}(B \to K_0^* \ell^+ \ell^-) &= -\frac{G_F \alpha}{4\sqrt{2}\pi} V_{tb} V_{ts}^* \{\bar{\ell}\gamma^\mu \ell [A(p_B + p_{K_0^*})_\mu + B q_\mu] \\ &\quad + \bar{\ell}\gamma^\mu \gamma_5 \ell [C(p_B + p_{K_0^*})_\mu + D q_\mu] + \bar{\ell}\ell Q + \bar{\ell}\gamma_5 \ell N\}.\end{aligned} \tag{16}$$

The functions entering Eq. (16) are defined as

$$\begin{aligned}A &= -(C_{LL} + C_{LR}) f_+ + 2(C_{BR} - C_{SL}) \frac{f_T}{m_B + m_{K_0^*}}, \\ B &= -(C_{LL} + C_{LR}) f_- - 2(C_{BR} - C_{SL}) \frac{f_T}{(m_B + m_{K_0^*}) q^2} \\ &\quad \times (m_B^2 - m_{K_0^*}^2), \\ C &= -(C_{LR} - C_{LL}) f_+, \qquad D = -(C_{LR} - C_{LL}) f_-, \\ Q &= -f_0 \frac{m_B^2 - m_{K_0^*}^2}{m_b + m_s} (C_{LRLR} + C_{RLLR} + C_{LRRL} + C_{RLRL}), \\ N &= -f_0 \frac{m_B^2 - m_{K_0^*}^2}{m_b + m_s} (C_{LRLR} + C_{RLLR} - C_{LRRL} - C_{RLRL}),\end{aligned} \tag{17}$$

where

$$\begin{aligned}C_{LL} &= (\tilde{C}_9^{\text{eff}} - \tilde{C}_{10}), \qquad C_{LR} = (\tilde{C}_9^{\text{eff}} + \tilde{C}_{10}), \\ C_{SL} &= -2 m_s C_7^{\text{eff}}, \qquad C_{BR} = -2 m_b C_7^{\text{eff}}, \\ C_{LRLR} &= C_{Q_1} + C_{Q_2}, \qquad C_{LRRL} = C_{Q_1} - C_{Q_2}, \\ C_{RLLR} &= C_{RLRL} = 0.\end{aligned} \tag{18}$$

In the present work, we use the three-point QCD-sum-rules predictions for the relevant form factors of the $B \to K_0^*$ transition, in which the form factors

$$F(q^2) \in \{f_+(q^2), f_-(q^2), f_T(q^2)\}$$

are fitted to the following functions [31]:

$$F(q^2) = \frac{F(0)}{1 - a_F \frac{q^2}{m_B^2} + b_F \left(\frac{q^2}{m_B^2}\right)^2}, \tag{19}$$

where the parameters $F(0)$, a_F, and b_F are listed in Table I. From the expression of the matrix element given in Eq. (16), we get the following result for the differential decay with:

$$\frac{d\Gamma}{d\hat{s}}(B \to K_0^* \ell^+ \ell^-) = \frac{G^2 \alpha^2 m_B}{2^{14} \pi^5} |V_{tb} V_{ts}^*|^2 \lambda^{1/2}(1, \hat{r}_{K_0^*}, \hat{s}) v \Delta(\hat{s}), \tag{20}$$

TABLE I. Parameters entering the fit parametrization of the form factors for the $B \to K_0^*(1430)$ transition [31].

	$F(0)$	a_F	b_F
$f_+^{B \to K_0^*}$	0.31 ± 0.08	0.81	-0.21
$f_-^{B \to K_0^*}$	-0.31 ± 0.07	0.80	-0.36
$f_T^{B \to K_0^*}$	-0.26 ± 0.07	0.41	-0.32

where $\lambda(1, \hat{r}_{K_0^*}, \hat{s}) = 1 + \hat{r}_{K_0^*}^2 + \hat{s}^2 - 2\hat{r}_{K_0^*} - 2\hat{s} - 2\hat{r}_{K_0^*}\hat{s}$, $\hat{s} = q^2/m_B^2$, $\hat{r}_{K_0^*} = m_{K_0^*}^2/m_B^2$, $\hat{m}_\ell = m_\ell/m_B$, and $v = \sqrt{1 - 4\hat{m}_\ell^2/\hat{s}}$ is the final lepton velocity. Also, $\Delta(\hat{s})$ is

$$\begin{aligned}\Delta = \frac{4m_B^2}{3} \text{Re}[&+24 m_B^2 \hat{m}_\ell^2 (1 - \hat{r}_{K_0^*})(CD^*) \\ &+ 12 m_B \hat{m}_\ell (1 - \hat{r}_{K_0^*})(CN^*) + 12 m_B^2 \hat{m}_\ell^2 \hat{s} |D|^2 \\ &+ 3\hat{s}|N|^2 + 12 m_B \hat{m}_\ell \hat{s}(DN^*) + \lambda m_B^2 (3 - v^2)|A|^2 \\ &+ 3\hat{s} v^2 |Q|^2 + m_B^2 \{2\lambda - (1 - v^2)[2\lambda - 3(1 - \hat{r}_{K_0^*})^2]\}|C|^2].\end{aligned} \tag{21}$$

We now proceed by calculating the double-polarization asymmetries, i.e., when polarizations of both leptons are simultaneously measured. We introduce a spin projection operator defined by

$$\Lambda_1 = \tfrac{1}{2}(1 + \gamma_5 \not{s}_i^-), \qquad \Lambda_2 = \tfrac{1}{2}(1 + \gamma_5 \not{s}_i^+)$$

for lepton ℓ^- and antilepton ℓ^+, where $i = L, N, T$ are the abbreviations of longitudinal, normal, and transversal polarizations, respectively. Firstly, we define the following orthogonal unit vectors $s^{-\mu}$ in the rest frame of ℓ^- and $s^{+\mu}$ in the rest frame of ℓ^+:

$$\begin{aligned}s_L^{-\mu} &= (0, \vec{e}_L^-) = \left(0, \frac{\vec{p}_-}{|\vec{p}_-|}\right), \\ s_N^{-\mu} &= (0, \vec{e}_N^-) = \left(0, \frac{\vec{p}_{K_0^*} \times \vec{p}_-}{|\vec{p}_{K_0^*} \times \vec{p}_-|}\right), \\ s_T^{-\mu} &= (0, \vec{e}_T^-) = (0, \vec{e}_N^- \times \vec{e}_L^-), \\ s_L^{+\mu} &= (0, \vec{e}_L^+) = \left(0, \frac{\vec{p}_+}{|\vec{p}_+|}\right), \\ s_N^{+\mu} &= (0, \vec{e}_N^+) = \left(0, \frac{\vec{p}_{K_0^*} \times \vec{p}_+}{|\vec{p}_{K_0^*} \times \vec{p}_+|}\right), \\ s_T^{+\mu} &= (0, \vec{e}_T^+) = (0, \vec{e}_N^+ \times \vec{e}_L^+),\end{aligned} \tag{22}$$

where $\vec{p}_\mp$ and $\vec{p}_{K_0^*}$ are the three-momenta of the leptons $\ell^\mp$ and K_0^* meson in the center-of-mass frame (CM) of the $\ell^- \ell^+$ system, respectively. By using Lorentz transformation, we boost the unit vectors from the rest frame of leptons to the CM frame of leptons. While the vector $s_L^{\mp\mu}$ changes as

$$(s_L^{-\mu})_{\rm CM} = \left(\frac{|\vec{p}_-|}{m_\ell}, \frac{E\vec{p}_-}{m_\ell|\vec{p}_-|}\right), \qquad (s_L^{+\mu})_{\rm CM} = \left(\frac{|\vec{p}_-|}{m_\ell}, -\frac{E\vec{p}_-}{m_\ell|\vec{p}_-|}\right), \tag{23}$$

the other two unit vectors $s_N^{\mp\mu}$ and $s_T^{\mp\mu}$ remain unchanged.

We can now define the double-lepton polarization asymmetries as [30]:

$$P_{ij}(\hat{s}) = \frac{(\frac{d\Gamma}{d\hat{s}}(\vec{s}_i^-, \vec{s}_j^+) - \frac{d\Gamma}{d\hat{s}}(-\vec{s}_i^-, \vec{s}_j^+)) - (\frac{d\Gamma}{d\hat{s}}(\vec{s}_i^-, -\vec{s}_j^+) - \frac{d\Gamma}{d\hat{s}}(-\vec{s}_i^-, -\vec{s}_j^+))}{(\frac{d\Gamma}{d\hat{s}}(\vec{s}_i^-, \vec{s}_j^+) + \frac{d\Gamma}{d\hat{s}}(-\vec{s}_i^-, \vec{s}_j^+)) + (\frac{d\Gamma}{d\hat{s}}(\vec{s}_i^-, -\vec{s}_j^+) + \frac{d\Gamma}{d\hat{s}}(-\vec{s}_i^-, -\vec{s}_j^+))}, \tag{24}$$

where $i, j = L, N, T$; the first subindex i corresponds to the lepton while the second subindex j corresponds to the antilepton, respectively. After doing calculations, we get the following results for the double-polarization asymmetries:

$$\begin{aligned} P_{LL} = \frac{4m_B^2}{3\Delta}\,\mathrm{Re}[&+24m_B^2\hat{m}_\ell^2(1-\hat{r}_{K_0^*})(C^*D) + 12m_B\hat{m}_\ell(1-\hat{r}_{K_0^*})(C^*N) - \lambda m_B^2(1+v^2)|A|^2 + 12m_B^2\hat{m}_\ell^2\hat{s}|D|^2 + 3\hat{s}|N|^2 \\ &+ 12m_B\hat{m}_\ell\hat{s}(D^*N) + 3\hat{s}v^2|Q|^2 - m_B^2\{2\lambda - (1-v^2)[2\lambda + 3(1-\hat{r}_{K_0^*})^2]\}|C|^2], \end{aligned} \tag{25}$$

$$P_{LN} = \frac{2\pi m_B^3\sqrt{\lambda\hat{s}}}{\hat{s}\Delta}\,\mathrm{Im}[2m_B\hat{m}_\ell\hat{s}\,\mathrm{Im}(A^*D) + \hat{s}(A^*N) - \hat{s}v^2(C^*Q) + 2m_B\hat{m}_\ell(1-\hat{r}_{K_0^*})(A^*C)], \tag{26}$$

$$P_{NL} = \frac{2\pi m_B^3\sqrt{\lambda\hat{s}}}{\hat{s}\Delta}\,\mathrm{Im}[-2m_B\hat{m}_\ell\hat{s}(A^*D) - \hat{s}(A^*N) + \hat{s}v^2(C^*Q) - 2m_B\hat{m}_\ell(1-\hat{r}_{K_0^*})(A^*C)], \tag{27}$$

$$P_{LT} = \frac{2\pi m_B^3\sqrt{\lambda\hat{s}}}{\hat{s}\Delta}\,\mathrm{Re}[2m_B\hat{m}_\ell(1-\hat{r}_{K_0^*})v|C|^2 + 2m_B\hat{m}_\ell\hat{s}v(C^*D) + \hat{s}v(C^*N) - \hat{s}v(A^*Q)], \tag{28}$$

$$P_{TL} = \frac{2\pi m_B^3\sqrt{\lambda\hat{s}}}{\hat{s}\Delta}\,\mathrm{Re}[2m_B\hat{m}_\ell(1-\hat{r}_{K_0^*})v|C|^2 + 2m_B\hat{m}_\ell\hat{s}v(C^*D) + \hat{s}v(C^*N) + \hat{s}v(A^*Q)], \tag{29}$$

$$P_{NT} = \frac{8m_B^2 v}{3\Delta}\,\mathrm{Im}[+6m_B\hat{m}_\ell\hat{s}(D^*Q) + 3\hat{s}(N^*Q) - 2\lambda m_B^2(A^*C) + 6m_B\hat{m}_\ell(1-\hat{r}_{K_0^*})(C^*Q)], \tag{30}$$

$$P_{TN} = \frac{8m_B^2 v}{3\Delta}\,\mathrm{Im}[+6m_B\hat{m}_\ell\hat{s}(D^*Q) + 3\hat{s}(N^*Q) + 2\lambda m_B^2(A^*C) + 6m_B\hat{m}_\ell(1-\hat{r}_{K_0^*})(C^*Q)], \tag{31}$$

$$\begin{aligned} P_{TT} = \frac{4m_B^2}{3\Delta}\,\mathrm{Re}[&-24m_B^2\hat{m}_\ell^2(1-\hat{r}_{K_0^*})(C^*D) - 12m_B\hat{m}_\ell(1-\hat{r}_{K_0^*})(C^*N) - \lambda m_B^2(1+v^2)|A|^2 - 12m_B^2\hat{m}_\ell^2\hat{s}|D|^2 \\ &- 3\hat{s}|N|^2 - 12m_B\hat{m}_\ell\hat{s}(D^*N) + 3\hat{s}v^2|Q|^2 + m_B^2\{2\lambda - (1-v^2)[2\lambda + 3(1-\hat{r}_{K_0^*})^2]\}|C|^2], \end{aligned} \tag{32}$$

$$\begin{aligned} P_{NN} = \frac{4m_B^2}{3\Delta}\,\mathrm{Re}[&-3\hat{s}v^2|Q|^2 + 12m_B^2\hat{m}_\ell^2\hat{s}|D|^2 + 3\hat{s}|N|^2 + 12m_B\hat{m}_\ell\hat{s}(D^*N) - \lambda m_B^2(3-v^2)|A|^2 \\ &+ m_B^2\{2\lambda - (1-v^2)[2\lambda - 3(1-\hat{r}_{K_0^*})^2]\}|C|^2 + 24m_B^2\hat{m}_\ell^2(1-\hat{r}_{K_0^*})(C^*D) + 12m_B\hat{m}_\ell(1-\hat{r}_{K_0^*})(C^*N)]. \end{aligned} \tag{33}$$

III. RESULTS AND DISCUSSIONS

In this section, the q^2 dependence of the double-lepton polarization asymmetries as well as the average of these quantities over q^2, which is defined by

$$\langle P_{ij}\rangle = \frac{\int_{4\hat{m}_\ell^2}^{(1-\sqrt{\hat{r}_{K_0^*}})^2} P_{ij}\frac{d\mathcal{B}}{d\hat{s}}d\hat{s}}{\int_{4\hat{m}_\ell^2}^{(1-\sqrt{\hat{r}_{K_0^*}})^2}\frac{d\mathcal{B}}{d\hat{s}}d\hat{s}}, \tag{34}$$

on the parameters of model III 2HDM are studied. The full kinematical interval of the dilepton invariant mass q^2 is $4m_\ell^2 \leq q^2 \leq (m_B - m_{K_0^*})^2$, for which the long-distance effects (the charmonium resonances) can give significant contribution by including the first and second resonances J/ψ and ψ', in the interval of 8 GeV$^2 \leq q^2 \leq 14$ GeV^2. In order to reduce the hadronic uncertainties, we divide the kinematical region of q^2 for muon as

$$\begin{aligned} &\text{I} \quad 4m_\ell^2 \leq q^2 \leq (m_{J\psi} - 0.02\ \text{GeV})^2, \\ &\text{II} \quad (m_{J\psi} + 0.02\ \text{GeV})^2 \leq q^2 \leq (m_{\psi'} - 0.02\ \text{GeV})^2, \\ &\text{III} \quad (m_{\psi'} + 0.02\ \text{GeV})^2 \leq q^2 \leq (m_B - m_{K_0^*})^2, \end{aligned}$$

and for tau as

$$\begin{aligned} &\text{I} \quad 4m_\ell^2 \leq q^2 \leq (m_{\psi'} - 0.02\ \text{GeV})^2, \\ &\text{II} \quad (m_{\psi'} + 0.02\ \text{GeV})^2 \leq q^2 \leq (m_B - m_{K_0^*})^2. \end{aligned}$$

Since in model III 2HDM λ_{tt} and λ_{bb} can be complex parameters, we can rewrite the following product as

$$\lambda_{tt}\lambda_{bb} \equiv |\lambda_{tt}\lambda_{bb}|e^{i\theta}, \tag{35}$$

where $|\lambda_{tt}|$, $|\lambda_{bb}|$, and the phase angle θ are restricted by the experimental results of the electric dipole moments of neutron, $B^0 - \bar{B}^0$ mixing, ρ_0, R_b, and Br$(b \to s\gamma)$ [21–24]. The experimental limits on the electric dipole moments of neutron and Br$(b \to s\gamma)$, plus M_{H^+}, which is obtained at LEPII, put constraints on $\lambda_{tt}\lambda_{bb}$ to be nearly 1 and the phase angle θ to be in the interval between 60°–90°. The experimental value of the x_d parameter, relating to $B^0 - \bar{B}^0$ mixing, imposes the following condition on $|\lambda_{tt}|$, which is $|\lambda_{tt}| \leq 0.3$. Also, the parameter R_b, which is defined as $R_b \equiv \frac{\Gamma(Z \to b\bar{b})}{\Gamma(Z \to \text{hadrons})}$, keeps $|\lambda_{bb}|$ approximately fixed, $|\lambda_{bb}| \simeq 50$. Using these restrictions and taking $\theta = \pi/2$, we consider the following three typical parameter spaces throughout the numerical analysis:

$$\begin{aligned} &\text{Case A: } |\lambda_{tt}| = 0.03; \qquad |\lambda_{bb}| = 100, \\ &\text{Case B: } |\lambda_{tt}| = 0.15; \qquad |\lambda_{bb}| = 50, \\ &\text{Case C: } |\lambda_{tt}| = 0.3; \qquad |\lambda_{bb}| = 30. \end{aligned} \tag{36}$$

In addition, in our numerical analysis, we have used two sets of masses of Higgs bosons, which are displayed in Table II. For form factors, as pointed out in Sec. II, we have chosen the predictions of three-point QCD sum rules method [31], and for the other input parameters, we have used the following values [32]:

TABLE II. List of the values for the masses of the Higgs particles.

	m_{A^0}	m_{h^0}	m_{H^0}	$m_{H^\pm}$
mass set 1	120 GeV	115 GeV	160 GeV	200 GeV
mass set 2	95 GeV	100 GeV	125 GeV	160 GeV

$$\begin{aligned} &m_B = 5.279 \pm 0.03\ \text{GeV}, \qquad m_{K_0^*} = 1.425 \pm 0.05\ \text{GeV}, \\ &m_b = 4.19^{+0.18}_{-0.06}\ \text{GeV}, \qquad m_c = 1.27^{+0.07}_{-0.09}\ \text{GeV}, \\ &m_s = 0.101^{+0.029}_{-0.021}\ \text{GeV}, \qquad m_\mu = 0.105\ \text{GeV}, \\ &m_\tau = 1.77\ \text{GeV}, \qquad \alpha^{-1} = 129, \\ &\tau_B = (1.525 \pm 0.009) \times 10^{-12}\ \text{s}, \\ &\lambda = 0.2253 \pm 0.0007, \qquad A = 0.808^{+0.022}_{-0.015}, \\ &\bar{\rho} = 0.132^{+0.022}_{-0.014}, \qquad \bar{\eta} = 0.341 \pm 0.013, \end{aligned} \tag{37}$$

where A, λ, $\bar{\rho}$, $\bar{\eta}$ are the Wolfenstein parameters in the Cabibbo-Kobayashi-Maskawa matrix.

We have presented our analysis for the dependency of P_{ij} on the dilepton invariant mass, q^2, and the model III 2HDM parameters in a series of figures (see Figs. 1–7). In addition, by considering the theoretical and experimental uncertainties for the average of double-lepton polarization asymmetries in $B \to K_0^* \ell^+ \ell^-$ decay in the SM, the effects of model III 2HDM parameters for both mass sets of Higgs bosons were studied on the mentioned asymmetries in Tables III and IV. Besides, as it was stated in the introduction, for each asymmetry, we have compared our results with those of SM4 [6] and ACDM [25]. It should be mentioned finally that the theoretical uncertainties come from the hadronic uncertainties related to the form factors, and the experimental uncertainties originate from the mass of quarks, hadrons, and Wolfenstein parameters.

(i) Figure 1 and Tables III and IV: As it is seen from this figure, the dependency of P_{LL} on q^2 for the μ channel in the SM and 2HDM, to a large extent, is the same, such that the tree plots of 2HDM concerning each mass set of Higgs bosons coincide with the SM plot. In the τ channel, the dependency of this asymmetry on the mass sets of Higgs bosons is more observed, such that the maximum deviation from the SM value, which is about 20% SM, happens in the case C of mass set 2 at $q^2 = 4m_\tau^2$. It is also obvious from Tables III and IV that the magnitude of $\langle P_{LL} \rangle$ in 2HDM for the μ channel and τ channel is in the range of SM prediction. The comparison of the results of this article for P_{LL} and its averages in the μ channel and τ channel with those of Ref. [6,25] indicate that this asymmetry for all these models lies in the range of SM anticipation, and the results of these models show no significant differences from each other.

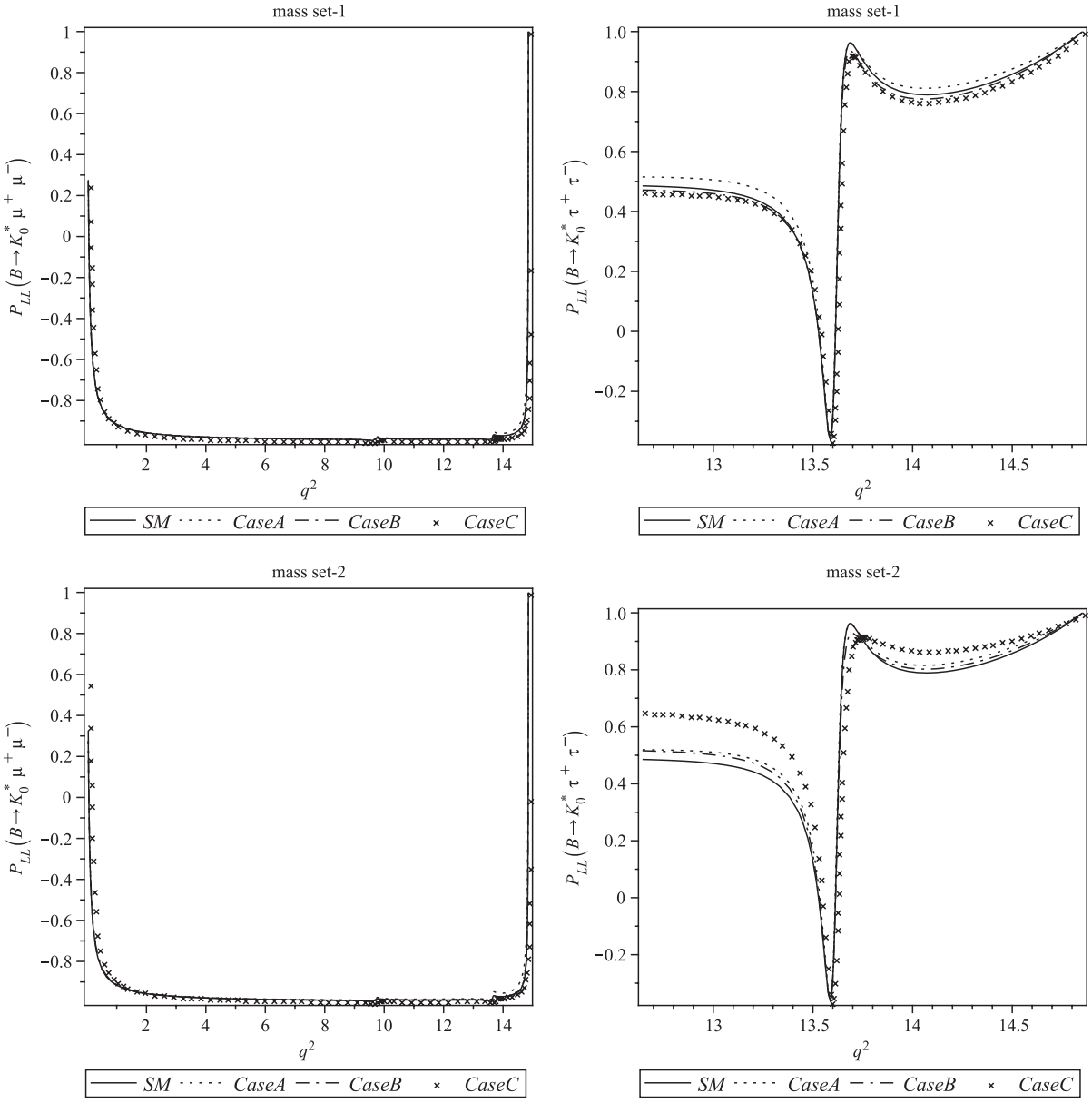

FIG. 1. The dependence of the P_{LL} polarization on q^2 for both mass sets of Higgs bosons (mass set 1 and mass set 2) and three typical cases of 2HDM, i.e. cases A, B, and C, and the SM for the μ and τ channels. Case A refers to $\theta = \pi/2$, $|\lambda_{tt}| = 0.03$, and $|\lambda_{bb}| = 100$. Case B refers to $\theta = \pi/2$, $|\lambda_{tt}| = 0.15$, and $|\lambda_{bb}| = 50$. Case C refers to $\theta = \pi/2$, $|\lambda_{tt}| = 0.3$, and $|\lambda_{bb}| = 30$.

(ii) Figure 2 and Tables III and IV: It is seen from Eqs. (26) and (27) that, in both SM and 2HDM, P_{LN} is an antisymmetric quantity under the exchange of L and N, i.e. $P_{LN} = -P_{NL}$. Therefore, we only investigate the dependency of P_{LN} on q^2 and 2HDM parameters in the SM and 2HDM. From these plots, it is apparent that, although for both mass sets of Higgs bosons and both ranges $4m_\mu^2 \le q^2 \le 4m_\psi^2$ and $4m_\psi^2 < q^2 \le (m_B - m_{K_0^*})^2$ for the μ channel and both ranges $4m_\tau^2 \le q^2 \le 4m_{\psi'}^2$ and $4m_{\psi'}^2 < q^2 \le (m_B - m_{K_0^*})^2$ for the τ channel, as $|\lambda_{tt}\lambda_{bb}|$ and $|\lambda_{tt}|^2$ increase, the differences between the predictions of the SM and 2HDM get larger, the deviation from the SM value for the range $4m_\mu^2 \le q^2 \le 4m_\psi^2$ for the μ channel in the mass set 2 and for the range $4m_\tau^2 \le q^2 \le 4m_{\psi'}^2$ for the τ channel in the same mass set is more than the other considered cases. For example, while the magnitude of P_{LN} in the SM for the μ channel in $4m_\mu^2 \le q^2 \le 4m_\psi^2$ is about 0.01 and for the τ channel in $4m_\tau^2 \le q^2 \le 4m_{\psi'}^2$ is about 0.05, it reaches, at most, 0.35 (3400% SM) at $q^2 = 4m_\mu^2$ for μ channel and 0.28 (460% SM) at $q^2 = 4m_\tau^2$ for the τ channel in case C of the model III 2HDM in

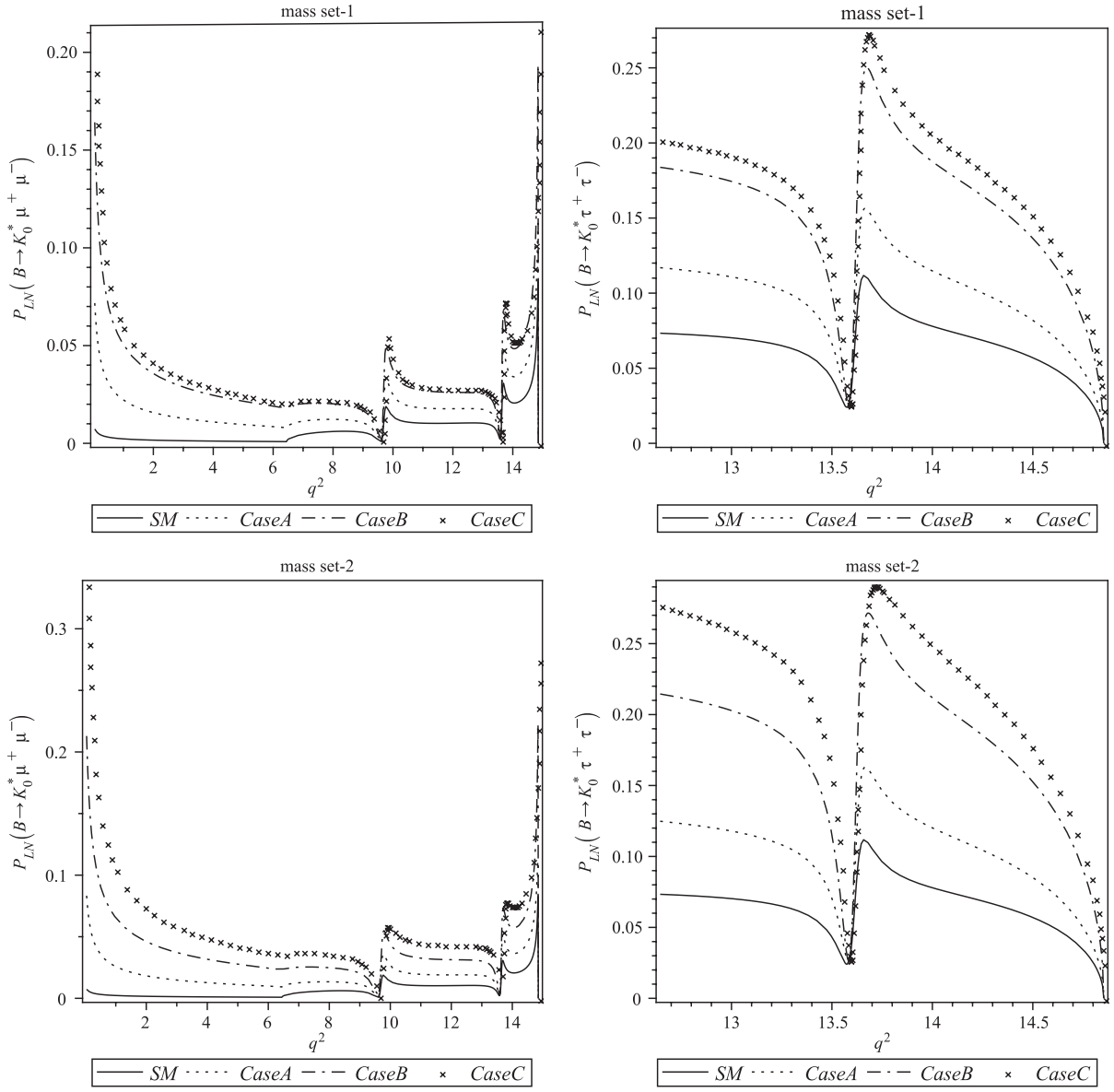

FIG. 2. The dependence of the P_{LN} polarization on q^2 for both mass sets of Higgs bosons (mass set 1 and mass set 2) and three typical cases of 2HDM, i.e. cases A, B, and C, and the SM for the μ and τ channels. Case A refers to $\theta = \pi/2$, $|\lambda_{tt}| = 0.03$, and $|\lambda_{bb}| = 100$. Case B refers to $\theta = \pi/2$, $|\lambda_{tt}| = 0.15$, and $|\lambda_{bb}| = 50$. Case C refers to $\theta = \pi/2$, $|\lambda_{tt}| = 0.3$, and $|\lambda_{bb}| = 30$.

mass set 2. Also, from these plots, it is found out that, whereas P_{LN} around the mass of resonances ψ and ψ' in the μ channel and around the mass of resonance ψ' in the τ channel shows sensitivity to the parameters of cases A, B, and C, it does not show such sensitivity to the changes of masses of Higgs bosons in mass set 1 and mass set 2. It is also obvious from Tables III and IV that, except in case A of mass set 1 for the μ channel, the SM value of $\langle P_{LN}\rangle$, which is in the intervals $0.014 \leq \langle P_{LN}\rangle \leq 0.016$ for the μ case and $0.050 \leq \langle P_{LN}\rangle \leq 0.085$ for the τ case, does not overlap with the predictions of 2HDM for these channels. By comparing the data of $\langle P_{LN}\rangle$ of Table III and IV with the data points of $\langle P_{LN}\rangle$ plots in Ref. [6] for SM4, it is understood that $\langle P_{LN}\rangle$ indicates more sensitivity to the fourth-generation parameters relative to the parameters of 2HDM, such that while there is a deviation of around 3350% SM for the μ case and a deviation of around 333% SM for the τ case in SM4, there exists a deviation of around 300% SM for the μ channel and a deviation around 243% SM for the τ channel in 2HDM. Also, it is clear from this article and Ref. [25] that the deviation of P_{LN} from SM in 2HDM is much more than that in ACDM. The estimation of the ACDM for P_{LN} in the τ case is at most -14% SM.

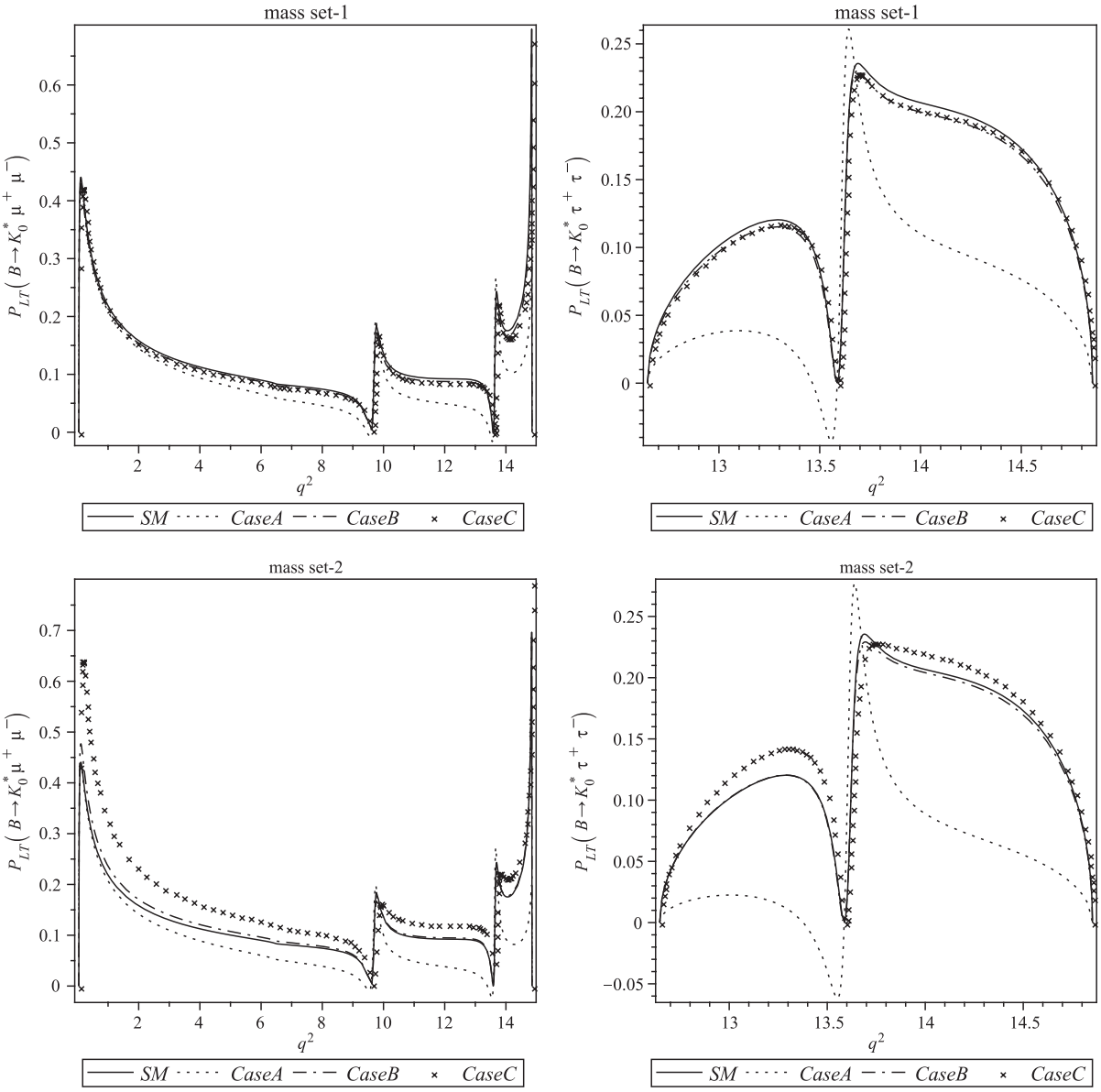

FIG. 3. The dependence of the P_{LT} polarization on q^2 for both mass sets of Higgs bosons (mass set 1 and mass set 2) and three typical cases of 2HDM, i.e. cases A, B, and C, and the SM for the μ and τ channels. Case A refers to $\theta = \pi/2$, $|\lambda_{tt}| = 0.03$, and $|\lambda_{bb}| = 100$. Case B refers to $\theta = \pi/2$, $|\lambda_{tt}| = 0.15$, and $|\lambda_{bb}| = 50$. Case C refers to $\theta = \pi/2$, $|\lambda_{tt}| = 0.3$, and $|\lambda_{bb}| = 30$.

(iii) Figures 3 and 4 and Tables III and IV: By comparing Eqs. (28) and (29), it is found out that P_{LT} is symmetric under the exchange of subscripts L and T in the SM for both the μ channel and τ channel, but it is neither symmetric nor antisymmetric under the exchange of those subscripts in 2HDM. Moreover, it is clear from Figs. 3 and 4 that for the μ channel in case C of model III 2HDM and for the τ channel in case A of model III 2HDM, a considerable discrepancy between the SM and 2HDM predictions occurs that reaches to, at most, 48% SM for the μ case of P_{LT} and P_{TL} and -100% SM and 100% SM for the τ case of P_{LT} and P_{TL}, respectively. Furthermore, as it is seen from these figures, both of these asymmetries show no strong dependency on the mass sets of Higgs bosons. It is also obvious from Table III that in the μ channel, the 2HDM values of $\langle P_{LT}\rangle$ and $\langle P_{TL}\rangle$ for cases A and C relating both mass sets of Higgs bosons cannot interfere with the SM expectations, which are $0.123 \leq \langle P_{LT}\rangle \leq 0.152$ and $0.123 \leq \langle P_{TL}\rangle \leq 0.152$. In addition, for the τ channel, it is understood from Table IV that the 2HDM values of $\langle P_{LT}\rangle$ and $\langle P_{TL}\rangle$ for case A cannot lie in the range of SM prediction, which is $0.093 \leq \langle P_{LT}\rangle \leq 0.187$ and $0.093 \leq \langle P_{TL}\rangle \leq 0.187$. From comparison of the results of this article for the averages of P_{LT} and P_{TL} in the μ channel with those in Ref. [6], it is

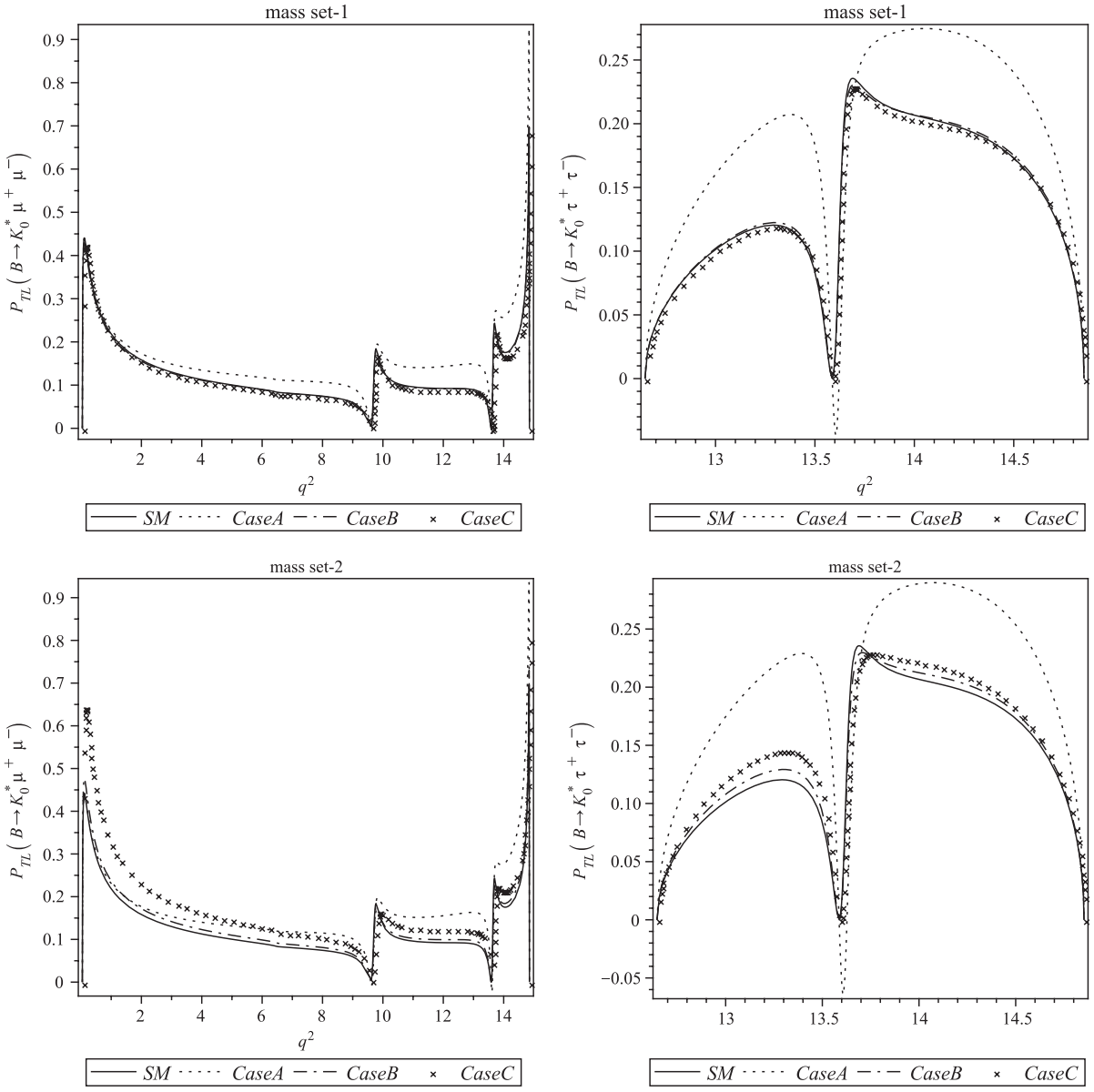

FIG. 4. The dependence of the P_{TL} polarization on q^2 for both mass sets of Higgs bosons (mass set 1 and mass set 2) and three typical cases of 2HDM, i.e. cases A, B, and C, and the SM for the μ and τ channels. Case A refers to $\theta = \pi/2$, $|\lambda_{tt}| = 0.03$, and $|\lambda_{bb}| = 100$. Case B refers to $\theta = \pi/2$, $|\lambda_{tt}| = 0.15$, and $|\lambda_{bb}| = 50$. Case C refers to $\theta = \pi/2$, $|\lambda_{tt}| = 0.3$, and $|\lambda_{bb}| = 30$.

inferred that in the μ channel, the fourth generation of quarks operates more impressively than the new Higgs bosons added to the SM so that, while the deviation of $\langle P_{LT}\rangle$ and $\langle P_{TL}\rangle$ from the SM in SM4 is almost 60% SM, it reaches to 42% SM in 2HDM. In contrast, from the similar comparison in the τ channel, it is understood that 2HDM shows considerable effects on these asymmetries, such that, while this model reduces $\langle P_{LT}\rangle$ around 69% SM and enhances $\langle P_{TL}\rangle$ around 69% SM, SM4 makes an increase of about 18% SM in the aforementioned asymmetries. It is also apparent from the plots regarding P_{LT} in Ref. [25] for the μ channel and τ channel, compared to those for 2HDM, the ACDM cannot cause an important difference between its predictions with that of the SM.

(iv) Figure 5 and Tables III and IV: Since only the parameters A and B, appearing in Eq. (17), have imaginary parts due to $\tilde{C}_9^{\text{eff}}$, it is understood that Eqs. (28) and (29) are antisymmetric under the exchange of N and T in both the SM and 2HDM, i.e. $P_{NT} = -P_{TN}$. Based on this, we only study the variations of P_{NT} in the SM and 2HDM with respect to q^2 and 2HDM parameters. From the μ channel of Fig. 5, it is easily seen that, first, for the whole range of $4m_\mu^2 < q^2 < (m_B - m_{K_0^*})^2$ in both mass sets of Higgs bosons, as $|\lambda_{tt}\lambda_{bb}|$ and $|\lambda_{tt}|^2$ increase, the difference between the magnitudes of

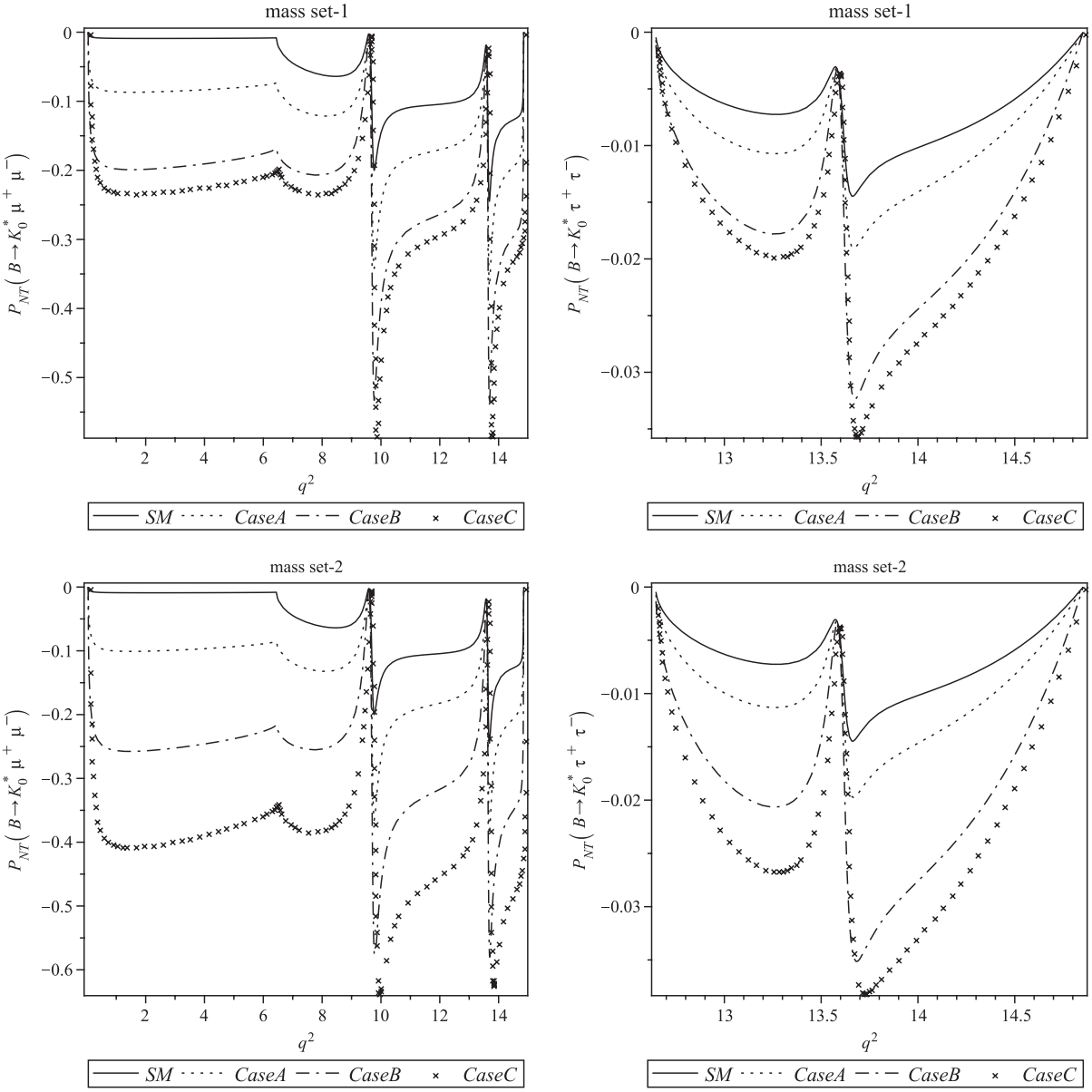

FIG. 5. The dependence of the P_{NT} polarization on q^2 for both mass sets of Higgs bosons (mass set 1 and mass set 2) and three typical cases of 2HDM, i.e. cases A, B, and C, and the SM for the μ and τ channels. Case A refers to $\theta = \pi/2$, $|\lambda_{tt}| = 0.03$, and $|\lambda_{bb}| = 100$. Case B refers to $\theta = \pi/2$, $|\lambda_{tt}| = 0.15$, and $|\lambda_{bb}| = 50$. Case C refers to $\theta = \pi/2$, $|\lambda_{tt}| = 0.3$, and $|\lambda_{bb}| = 30$.

predictions in the SM and 2HDM enhances, and, second, this difference is more significant in the second mass set of Higgs bosons. For example, for the interval $4m_\mu^2 < q^2 < 4m_c^2$, the magnitude of P_{NT} in the SM is approximately zero, but it becomes a nonzero value with a negative sign in the three cases of 2HDM (A, B and C), where the largest variation from the SM prediction ($P_{NT} \approx -0.4$) happens in case C of mass set 2. In addition, in the range $4m_c^2 < q^2 < (m_B - m_{K_0^*})^2$, the most variations of P_{NT} occur around the mass of resonances ψ and ψ' in case C of mass set 2, in which the magnitudes of the off-resonance peaks decrease to, at most, 225% SM and 156% SM, respectively. It is also obvious from Fig. 5 for the τ channel that, for the whole range of $4m_\tau^2 < q^2 < (m_B - m_{K_0^*})^2$, similar to the μ channel, first, in both mass sets of Higgs bosons when $|\lambda_{tt}\lambda_{bb}|$ and $|\lambda_{tt}|^2$ increase the discrepancy between the predictions of the SM and 2HDM enhances, and, second, this discrepancy gets larger in mass set 2. For instance, around the mass of resonance ψ' in case C of mass set 2, the magnitude of the off-resonance peak reduces to, at most, 164% SM, which is the highest deviation of this asymmetry from the SM prediction for the τ channel. Moreover, it is evident from Tables III and IV that, for both mass sets of Higgs bosons, the averages of $\langle P_{NT}\rangle$ in the μ channel for

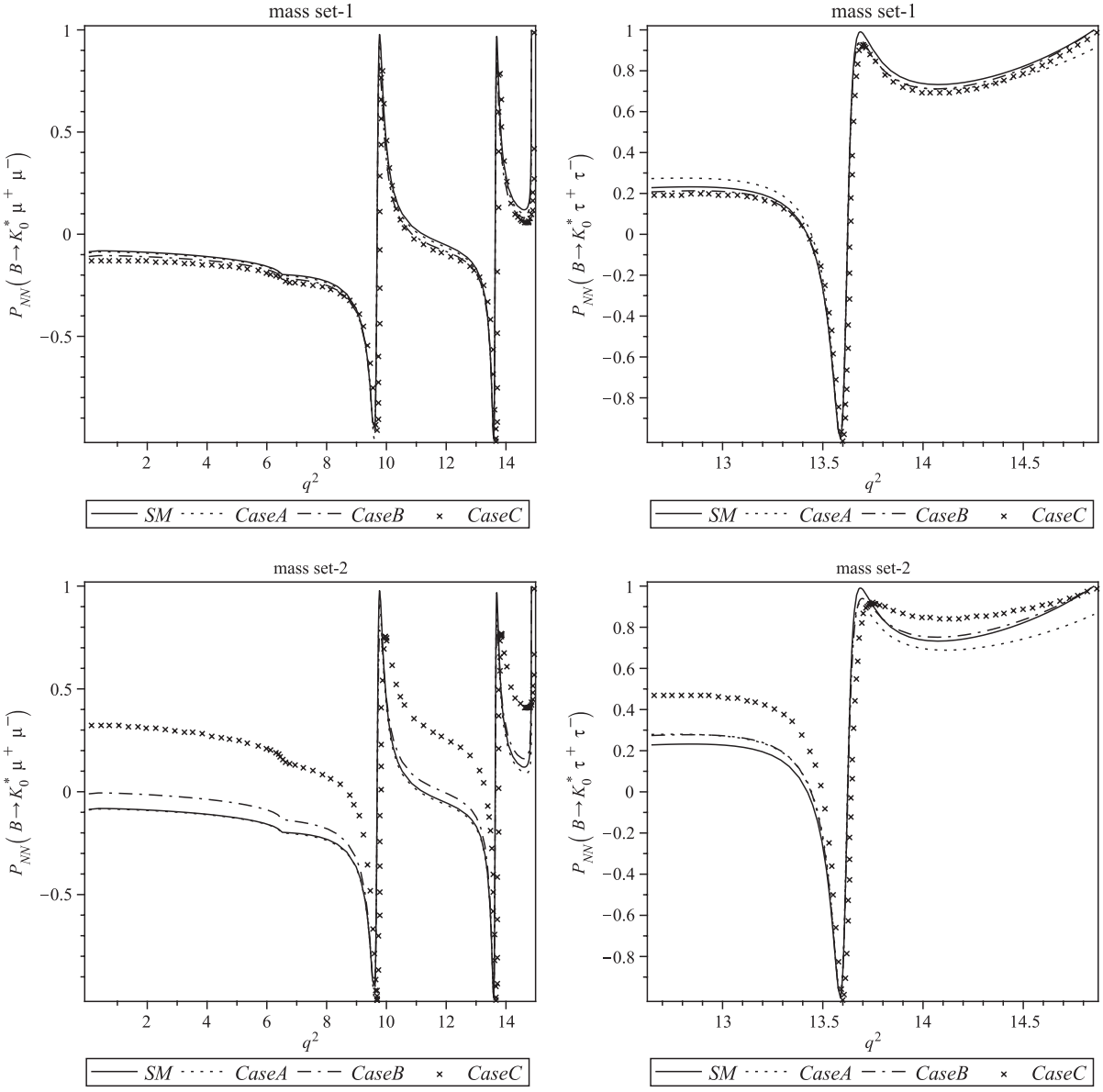

FIG. 6. The dependence of the P_{NN} polarization on q^2 for both mass sets of Higgs bosons (mass set 1 and mass set 2) and three typical cases of 2HDM, i.e. cases A, B, and C, and the SM for the μ and τ channels. Case A refers to $\theta = \pi/2$, $|\lambda_{tt}| = 0.03$, and $|\lambda_{bb}| = 100$. Case B refers to $\theta = \pi/2$, $|\lambda_{tt}| = 0.15$, and $|\lambda_{bb}| = 50$. Case C refers to $\theta = \pi/2$, $|\lambda_{tt}| = 0.3$, and $|\lambda_{bb}| = 30$.

the three cases, A, B, and C, and in the τ channel for cases B and C cannot overlap with the predictions of the SM by considering the lower limits of the corresponding SM uncertainties. From comparison of the results of this article for the averages of P_{NT} in the μ and τ channels with those in Ref. [6], it is found out that, in both channels, the fourth generation of quarks affects more intensively than the new Higgs bosons added to the SM, such that while the SM4 lowers $\langle P_{NT}\rangle$ by approximately 2100% SM in the μ case and 335% SM in the τ case, it gets down around 1315% SM for the μ channel and 257% SM for the τ channel in 2HDM. Besides, it is clear from the plots relating P_{NT} in Ref. [25] for the μ channel and τ channel that, in comparison with the similar plots in 2HDM, the ACDM cannot make an intensive difference between its predictions with those of the SM. This model causes an increase of around 8% SM for the μ channel and an increase around 50% SM for the τ channel.

(v) Figure 6 and Tables III and IV: As it is apparent from these curves, though, for the second mass set of Higgs bosons (mass set 2) and both intervals, $4m_\mu^2 \le q^2 \le 4m_\psi^2$ and $4m_\psi^2 < q^2 \le (m_B - m_{K_0^*})^2$ for the μ channel and both intervals $4m_\tau^2 \le q^2 \le 4m_{\psi'}^2$ and $4m_{\psi'}^2 < q^2 \le (m_B - m_{K_0^*})^2$ for the τ channel, when $|\lambda_{tt}\lambda_{bb}|$ and $|\lambda_{tt}|^2$ increase, the differences between the predictions of the SM and

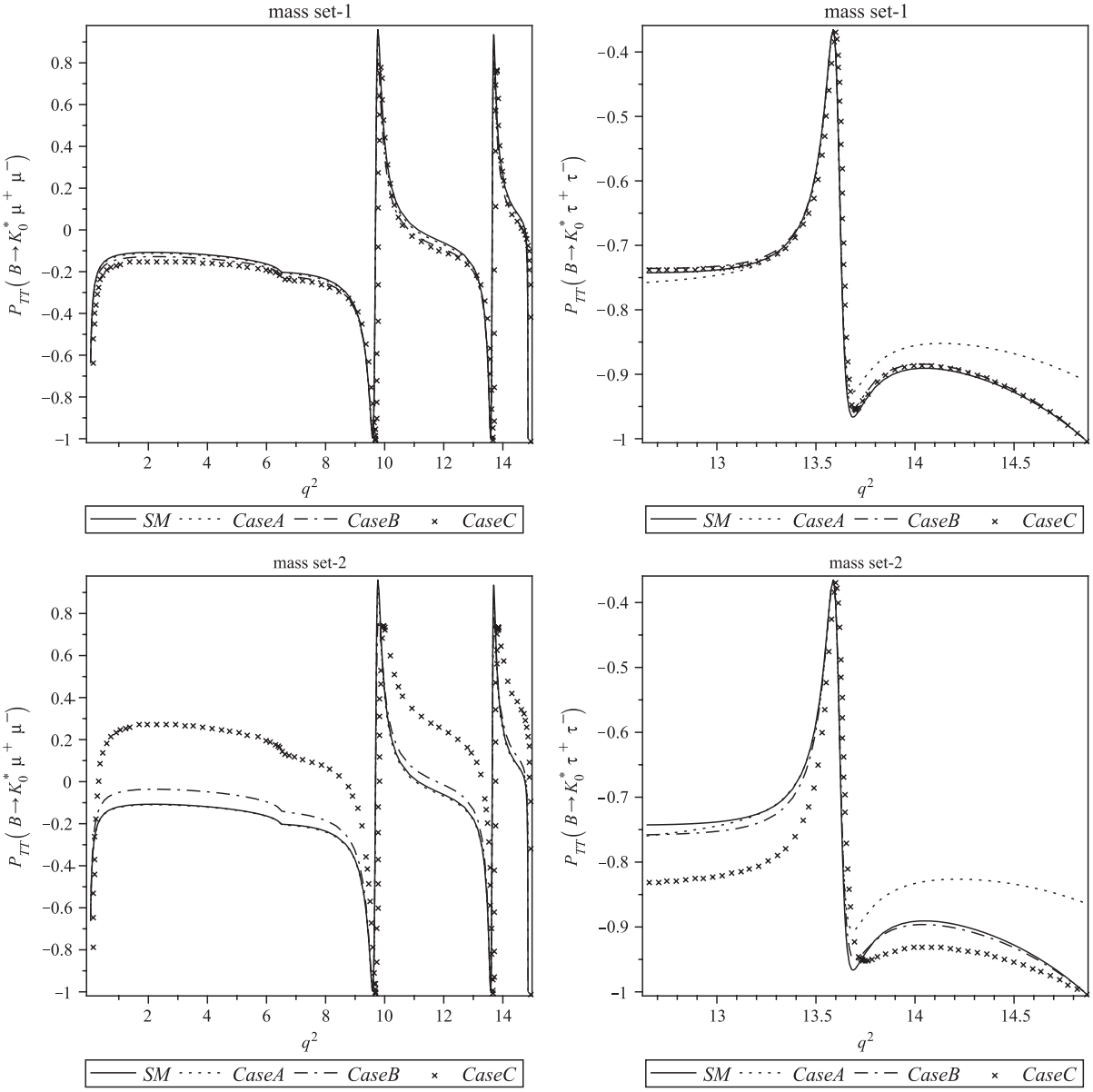

FIG. 7. The dependence of the P_{TT} polarization on q^2 for both mass sets of Higgs bosons (mass set 1 and mass set 2) and three typical cases of 2HDM, i.e. cases A, B, and C, and the SM for the μ and τ channels. Case A refers to $\theta = \pi/2$, $|\lambda_{tt}| = 0.03$, and $|\lambda_{bb}| = 100$. Case B refers to $\theta = \pi/2$, $|\lambda_{tt}| = 0.15$, and $|\lambda_{bb}| = 50$. Case C refers to $\theta = \pi/2$, $|\lambda_{tt}| = 0.3$, and $|\lambda_{bb}| = 30$.

2HDM enhance; the deviation from the SM value in the interval $4m_\mu^2 \le q^2 \le 4m_\psi^2$ for the μ channel and in the interval $4m_\tau^2 \le q^2 \le 4m_{\psi'}^2$ for the τ channel is more than the other investigated intervals. For example, for the magnitude of P_{NN} in case C of model III, there exists an increase of about 400% SM for the μ channel at $q^2 = 4m_\mu^2$ and a decrease of around 200% SM for the τ channel at $q^2 = 4m_\tau^2$. Also, from these plots, it is evident that, although the prediction of the SM for the range of $4m_\mu^2 \le q^2 \le 4m_\psi^2$ is negative, that of the model III 2HDM can be positive in case C. Moreover, it is apparent from this Figure that case C of mass set 2 causes the largest variations from the SM prediction in the on-resonance peaks, a reduction of around 20% SM for the μ channel and a reduction of nearly 10% SM for the τ channel. It is also obvious from Tables III and IV that the magnitudes of $\langle P_{NN}\rangle$ in 2HDM, except for cases B and C of mass set 2 for μ channel, lie in the range of the corresponding SM predictions. For instance, case C of mass set 2 in the μ channel can flip the sign of this asymmetry compared to that of the SM, which is negative. By comparing the data of $\langle P_{NN}\rangle$ of Table III with the corresponding data points of the $\langle P_{NN}\rangle$ plots in Ref. [6] for the μ channel in SM4, it is understood that $\langle P_{NN}\rangle$ shows more dependency on the

TABLE III. The averaged double-lepton polarization asymmetries for $B \to K_0^*(1430)\mu^+\mu^-$ in the SM and 2HDM for both mass sets of Higgs bosons (mass set 1 and mass set 2) and the three cases, A ($\theta = \pi/2$, $|\lambda_{tt}| = 0.03$ and $|\lambda_{bb}| = 100$), B ($\theta = \pi/2$, $|\lambda_{tt}| = 0.15$, and $|\lambda_{bb}| = 50$), and C ($\theta = \pi/2$, $|\lambda_{tt}| = 0.3$, and $|\lambda_{bb}| = 30$). The errors shown for each asymmetry are due to the theoretical and experimental uncertainties. The first ones are related to the theoretical uncertainties, and the second ones are due to experimental uncertainties. The theoretical uncertainties come from the hadronic uncertainties related to the form factors, and the experimental uncertainties originate from the mass of quarks, hadrons, and Wolfenstein parameters.

	SM	Case A (Set 1)	Case B (Set 1)	Case C (Set 1)	Case A (Set 2)	Case B (Set 2)	Case C (Set 2)
$\langle P_{LL}\rangle$	$-0.950^{+0.002+0.001}_{-0.003-0.001}$	−0.949	−0.950	−0.950	−0.948	−0.948	−0.939
$\langle P_{LN}\rangle$	$0.016^{+0.000+0.000}_{-0.001-0.001}$	0.016	0.033	0.038	0.018	0.042	0.064
$\langle P_{LT}\rangle$	$0.136^{+0.009+0.004}_{-0.013-0.003}$	0.116	0.132	0.132	0.111	0.146	0.194
$\langle P_{TL}\rangle$	$0.136^{+0.009+0.004}_{-0.013-0.003}$	0.159	0.134	0.132	0.165	0.148	0.194
$\langle P_{NT}\rangle$	$-0.027^{+0.001+0.004}_{-0.001-0.006}$	−0.097	−0.197	−0.226	−0.109	−0.250	−0.382
$\langle P_{NN}\rangle$	$-0.134^{+0.020+0.018}_{-0.026-0.018}$	−0.139	−0.154	−0.161	−0.137	−0.068	0.234
$\langle P_{TT}\rangle$	$-0.156^{+0.018+0.017}_{-0.023-0.017}$	−0.161	−0.175	−0.182	−0.159	−0.094	0.191

fourth-generation parameters relative to the parameters of 2HDM; a sensitivity of around 371% SM in SM4 and around 275% SM in 2HDM is seen. On the other hand, it is clear from the same comparison for the τ channel that SM4 and 2HDM affect similarly the average of P_{NN} by raising the SM expectations to around 45%. In addition, it is evident from this article and Ref. [25] that the deviation of P_{NN} from the SM in 2HDM, which is 400% SM for the μ channel and 100% SM for the τ channel, is approximately twice that in ΛCDM, which is 167% SM for the μ channel and 45% SM for the τ channel.

(vi) Figure 7 and Tables III and IV: It is obvious from this figure that the dependency of P_{TT} on q^2 in the SM and 2HDM are very similar to that of P_{NN} in the SM and 2HDM. However, there are also some differences. For example, for the μ channel, the maximum deviation from the SM anticipation, which is around 400% SM, occurs at $q^2 \sim 1$ GeV. In addition, it is seen for the τ channel that P_{TT} is sensitive to the 2HDM parameters in both mass sets of Higgs bosons and both ranges $4m_\tau^2 \le q^2 \le 4m_{\psi'}^2$ and $4m_{\psi'}^2 < q^2 \le (m_B - m_{K_0^*})^2$, such that, in the first interval, case C shows the largest deviations compared to the SM prediction of around 12% SM, and, in the second interval, case A indicates the most deviations from the SM expectation of around −15% SM. It is also evident from Tables III and IV that, similar to the μ channel, the amounts of $\langle P_{TT}\rangle$ in 2HDM, except for cases B and C of mass set 2 for the μ channel, lie in the range of the corresponding SM predictions. For instance, case C of mass set 2 in the μ channel can change the sign of this asymmetry in comparison with that of the SM, which is negative. From comparison of the results of this article for the averages of P_{TT} in the μ and τ channels with those in Ref. [6], it is deduced that, in the μ channel, the fourth generation of quarks operates more effectively than the new Higgs bosons added to the SM, such that, while the SM4 raises $\langle P_{TT}\rangle$ by approximately 375% SM in the μ case, the 2HDM enhances this value by 222% SM in this channel; but in the τ channel, both models behave identically and bring down $\langle P_{TT}\rangle$ to 10% SM. As a result, these models cannot make

TABLE IV. Same as Table III, except for $B \to K_0^*(1430)\tau^+\tau^-$.

	SM	Case A (Set 1)	Case B (Set 1)	Case C (Set 1)	Case A (Set 2)	Case B (Set 2)	Case C (Set 2)
$\langle P_{LL}\rangle$	$0.615^{+0.452+0.025}_{-0.175-0.029}$	0.649	0.603	0.600	0.655	0.638	0.741
$\langle P_{LN}\rangle$	$0.068^{+0.011+0.006}_{-0.012-0.006}$	0.104	0.166	0.183	0.109	0.191	0.233
$\langle P_{LT}\rangle$	$0.143^{+0.017+0.027}_{-0.024-0.026}$	0.063	0.138	0.140	0.045	0.142	0.161
$\langle P_{TL}\rangle$	$0.143^{+0.017+0.027}_{-0.024-0.026}$	0.209	0.144	0.142	0.224	0.150	0.162
$\langle P_{NT}\rangle$	$-0.007^{+0.008+0.002}_{-0.003-0.002}$	−0.010	−0.018	−0.020	−0.011	−0.020	−0.025
$\langle P_{NN}\rangle$	$0.455^{+0.641+0.028}_{-0.248-0.032}$	0.471	0.438	0.433	0.463	0.490	0.645
$\langle P_{TT}\rangle$	$-0.808^{+0.225+0.013}_{-0.087-0.015}$	−0.794	−0.803	−0.802	−0.780	−0.819	−0.867

intensive differences between their predictions with those of the SM in the τ channel for the averages of P_{TT}. Besides, it is clear from the plots relating P_{TT} in Ref. [25] for the μ channel and τ channel that, in comparison with the analogous plots in 2HDM, the ACDM operates less effectively than 2HDM in the μ case so that the ACDM prediction (180% SM) is approximately one half that of 2HDM (400% SM), and, in the τ case, the predictions of both models are almost the same (15% SM).

Finally, let us discuss briefly whether the lepton polarization asymmetries are measurable in experiments or not. Experimentally, for measuring an asymmetry $\langle P_{ij}\rangle$ of the decay with branching ratio $\mathcal{B}$ at $n\sigma$ level, the required number of events (i.e., the number of $B\bar{B}$) is given by the formula

$$N = \frac{n^2}{\mathcal{B}s_1 s_2 \langle P_{ij}\rangle^2},$$

where s_1 and s_2 are the efficiencies of the leptons. The values of the efficiencies of the τ leptons differ from 50% to 90% for their various decay modes [33], and the error in τ-lepton polarization is approximately 10–15% [34]. So, the error in measurements of the τ-lepton asymmetries is estimated to be about 20–30%, and the error in obtaining the number of events is about 50%.

Based on the above expression for N, in order to detect the lepton-polarization asymmetries in the μ and τ channels at 3σ level, the minimum number of required events are given by (the efficiency of τ lepton is considered 0.5),

(i) for $B \to K_0^* \mu^+ \mu^-$ decay,

$$N \sim \begin{cases} 10^{7(7)} & \text{for } \langle P_{LL}\rangle, \\ 10^{8(8)} & \text{for } (\langle P_{NT}\rangle, \langle P_{TN}\rangle), \\ 10^{8(9)} & \text{for } \langle P_{TT}\rangle, \\ 10^{9(8)} & \text{for } \langle P_{NN}\rangle, \\ 10^{9(9)} & \text{for } (\langle P_{LT}\rangle, \langle P_{TL}\rangle), \\ 10^{10(10)} & \text{for } (\langle P_{LN}\rangle, \langle P_{NL}\rangle), \end{cases}$$

(ii) for $B \to K_0^* \tau^+ \tau^-$ decay,

$$N \sim \begin{cases} 10^{10(10)} & \text{for } (\langle P_{LL}\rangle, \langle P_{NN}\rangle, \langle P_{TT}\rangle), \\ 10^{11(11)} & \text{for } (\langle P_{LN}\rangle, \langle P_{NL}\rangle, \langle P_{LT}\rangle, \langle P_{TL}\rangle), \\ 10^{13(13)} & \text{for } (\langle P_{NT}\rangle, \langle P_{TN}\rangle). \end{cases}$$

In the above expressions, the first power refers to the first choice of mass sets of Higgs bosons, and the second power denotes the second choice of mass sets of Higgs bosons. Comparison of the above values for N with the number of produced $B\bar{B}$ pairs at the LHC experiments, including ATLAS, CMS, and LHCb ($\sim 10^{12}$ per year) as well as that number of the Super-LHC experiments (supposed to be $\sim 10^{13}$ per year), shows that, for the μ channel, all double-lepton polarizations plus the corresponding averaged asymmetries and for the τ channel, probably P_{LL}, P_{NN}, P_{TT}, P_{LN}, P_{NL}, P_{LT}, and P_{TL} as well as the corresponding averaged polarizations, can be detected at the LHC and the Super Large Hadron Collider (SLHC). However, such comparison for the asymmetries P_{NT} and P_{TN} and their averages for the τ channel indicates that these asymmetries could be measured just at the SLHC experiments. It is worth mentioning that, although the muon polarization is measured for stationary muons, such experiments will be very hard to perform in the near future. The τ polarization can be studied by investigating the decay products of τ. The measurement of τ polarization in this respect is easier than the polarization of the muon.

IV. SUMMARY

In this paper, the sensitivity of P_{ij}'s on the dilepton invariant mass, q^2, and the model III 2HDM parameters for $B \to K_0^* \ell^+ \ell^-$ decay were investigated, and the results were compared to those of the SM and ACDM. Also, for this decay, the effects of model III 2HDM parameters on the averages of double-lepton polarization asymmetries, $\langle P_{ij}\rangle$'s, were studied, and, by taking into account the corresponding theoretical and experimental errors in the SM, the results of the SM and 2HDM were compared to each other. In addition, by comparing the averages of double-lepton polarization asymmetries in 2HDM to those of SM4, after obtaining the required number of events for detecting each asymmetry at the LHC or the SLHC, we presented a comprehensive discussion regarding the lepton polarizations of $B \to K_0^* \ell^+ \ell^-$ decay. In summary, the following conclusions were obtained:

(i) According to the above discussions regarding the P_{LL} and P_{TT}, the relevant averages, and the required number of events at the LHC for detecting each asymmetry, it is found that only P_{TT} in the μ channel has a chance to show a sign of the model III 2HDM.

(ii) From the preceding parts concerning P_{LT}, P_{TL}, P_{LN}, P_{NL}, P_{NN}, the corresponding averages for the μ channel and τ channel, and the constraints on the number of $B\bar{B}$ pairs produced at the LHC, it is obvious that all of these asymmetries can be suitable for searching the model III 2HDM.

(iii) From the previous explanations, it is clear that, although measuring the magnitude of P_{NT}, P_{TN}, $\langle P_{NT}\rangle$, and $\langle P_{TN}\rangle$ in both the μ channel and τ channel can be significant for discovering new physics, due to the required number of $B\bar{B}$ pairs at the LHC for sighting these asymmetries in the μ channel and τ channel, only the mentioned asymmetries in the μ case are suitable for such

achievement. However, if the SLHC starts to operate, the aforementioned asymmetries in the τ case can be helpful for such a discovery.

(iv) It is apparent from the figures that, although, in general, all these asymmetries show more sensitivity to the masses of Higgs bosons in mass set 2 than in those of mass set 1, in the asymmetry P_{NT} in the μ case, compared to the others, such a discrepancy is more evident.

(v) Our analyses regarding the asymmetries show that, in the μ case, the effects of SM4, 2HDM, and ACDM on all asymmetries except P_{LL} and in the τ case, only on P_{LN}, P_{LT}, and P_{NT}, obey the following arrangement: ACDM $<$ 2HDM $<$ SM4. For the τ case, such a relation for P_{TL} appears as ACDM$<$ SM4 $<$ 2HDM; for P_{NN}, appears as ACDM$<$ 2HDM $\sim$ SM4; and for P_{TT}, appears as ACDM $\sim$ 2HDM $\sim$ SM4, which lies in the range of the SM prediction. This arrangement for P_{LL} in the μ and τ cases is obtained as ACDM $\sim$ 2HDM $\sim$ SM4 $\sim$ SM.

In conclusion, we have shown that the new Higgs bosons in the general model III 2HDM with spontaneous *CP* violation can show some significant effects in the double-lepton polarization asymmetries of $B \to K_0^* \ell^+ \ell^-$ decay, which can be useful in the *B* factory experiments to test the SM and search for new physics with more precise measurements.

ACKNOWLEDGMENTS

The authors would like to thank V. Bashiry for his useful discussions. Support of the Research Council of Shiraz University is gratefully acknowledged.

[1] T. M. Aliev and M. Savci, Phys. Rev. D **60**, 014005 (1999).
[2] T. M. Aliev and M. Savci, Phys. Lett. B **481**, 275 (2000).
[3] V. Bashiry and F. Falahati, Phys. Rev. D **77**, 015001 (2008).
[4] V. Bashiry, S. M. Zebarjad, F. Falahati, and K. Azizi, J. Phys. G **35**, 065005 (2008).
[5] S. M. Zebarjad, F. Falahati, and H. Mehranfar, Phys. Rev. D **79**, 075006 (2009).
[6] F. Falahati and R. Khosravi, Phys. Rev. D **83**, 015010 (2011).
[7] V. Bashiry and K. Zeynali, J. High Energy Phys. 12 (2007) 055.
[8] C. H. V. Chang, D. Chang, and W. Y. Keung, Phys. Rev. D **61**, 053007 (2000).
[9] M. Ahmady, M. Nagashima, and A. Sugamoto, Phys. Rev. D **64**, 054011 (2001).
[10] M. R. Ahmady, F. Falahati, and S. M. Zebarjad, Acta Phys. Pol. B **40**, 2775 (2009).
[11] N. Arkani-Hamed, A. G. Cohen, E. Katz and A. E. Nelson, J. High Energy Phys. 07 (2002) 034.
[12] S. Chang and H. J. He, Phys. Lett. B **586**, 95 (2004).
[13] N. Arkani, S. Dimopoulos, and G. Dvali, Phys. Lett. B **429**, 263 (1998); Phys. Rev. D **59**, 086004 (1999).
[14] T. Appelquist, H. C. Cheng, and B. A. Dobrescu, Phys. Rev. D **64**, 035002 (2001).
[15] C. Csaki, Mod. Phys. Lett. A **11**, 599 (1996).
[16] S. Glashow and S. Weinberg, Phys. Rev. D **15**, 1958 (1977).
[17] D. B. Chao, K. Cheung, and W. Y. Keung, Phys. Rev. D **59**, 115006 (1999).
[18] Q. S. Yan, C. S. Huang, W. Liao, and s. H. Zhu, Phys. Rev. D **62**, 094023 (2000).
[19] C. S. Huang and X. H. Wu, Nucl. Phys. **B657**, 304 (2003).
[20] V. Bashiry and M. Bayar, Eur. Phys. J. C **61**, 451 (2009).
[21] D. Atwood, L. Reina, and A. Soni, Phys. Rev. D **55**, 3156 (1997).
[22] D. Bowser-Chao, K. Cheung, and Wai-Yee Keung, Phys. Rev. D **59**, 115006 (1999).
[23] C. S. Huang and S. H. Zhu, Phys. Rev. D **68**, 114020 (2003).
[24] Y. B. Dai, C. S. Huang, J. T. Li, and W. J. Li, Phys. Rev. D **67**, 096007 (2003).
[25] B. B. Sirvanli, K. Azizi, and Y. Ipekoglu, J. High Energy Phys. 01 (2011) 069.
[26] Y. B Dai, C. S Huang, and H. W Huang, Phys. Lett. B **390**, 257 (1997).
[27] B. Grinstein, M. J. Savage, and M. B. Wise, Nucl. Phys. **B319**, 271 (1989).
[28] A. J. Buras and M. Münz, Phys. Rev. D **52**, 186 (1995).
[29] F. Krüger and L. M. Sehgal, Phys. Lett. B **380**, 199 (1996).
[30] T. M. Aliev, V. Bashiry, and M. Savcı, Eur. Phys. J. C **35**, 197 (2004).
[31] T. M. Aliev, K. Azizi, and M. Savcı, Phys. Rev. D **76**, 074017 (2007).
[32] K. Nakamura *et al.* (Particle Data Group), J. Phys. G **37**, 075021 (2010).
[33] G. Abbiendi *et al.* (OPAL Collaboration), Phys. Lett. B **492**, 23 (2000).
[34] A. Rouge, Z. Phys. C **48**, 75 (1990); *Proceedings of the Workshop on τ Lepton Physics*, Orsay, France, 1990 (unpublished).